Superfast Laser Cooling

S. Machnes,[1] M. B. Plenio,[2,3] B. Reznik,[1] A. M. Steane,[4] and A. Retzker[2]

[1]*Department of Physics and Astronomy, Tel-Aviv University, Tel Aviv 69978, Israel*
[2]*Institut für Theoretische Physik, Universität Ulm, D-89069 Ulm, Germany*
[3]*QOLS, The Blackett Laboratory, Imperial College London, Prince Consort Road, SW7 2BW, United Kingdom*
[4]*Department of Physics, University of Oxford, Clarendon Laboratory, Parks Road, Oxford OX1 3PU, United Kingdom*
(Received 15 January 2010; published 6 May 2010)

Currently, laser cooling schemes are fundamentally based on the weak coupling regime. This requirement sets the trap frequency as an upper bound to the cooling rate. In this work we present a numerical study that shows the feasibility of cooling in the strong-coupling regime which then allows cooling rates that are faster than the trap frequency with experimentally feasible parameters. The scheme presented here can be applied to trapped atoms or ions as well as to mechanical oscillators. It can also cool medium sized ion chains close to the ground state.

Introduction.—Laser cooling is the main tool that enables the exploration of low temperature phenomena in atomic physics, in nano- and microsystems as well as the rapidly developing field of quantum technologies. Following the original ideas of Doppler cooling [1,2], laser cooling has taken a central role in the physics of cold atoms and the number of ideas and their sophistication is growing continuously. In the quest to propose cooling schemes that can cool to lower and lower temperatures at ever increasing rates the complexity and the efficiency of laser cooling has progressed a long way.

Two-level systems (TLS) admit the Doppler cooling limit. This limit can be overcome by the Sisyphus mechanism either for free [3,4] or trapped particles [5]. The recoil limit can be broken by higher level systems by velocity selective coherent population (VSCP) [6] trapping or by Raman cooling [7] for free particles, and in their analog for bound particles, dark state cooling [8], Raman side band cooling [9] and Robust cooling [10]. Cooling schemes for trapped particles can be applied for mechanical oscillators, as in the setups described in [11,12].

However, all such cooling schemes assume a weak coupling between the internal degrees of freedom (DOF) and the ion's external motional state so that there is a clear separation of time scales between the two, allowing adiabatic elimination of the faster of the two DOFs. For example, the resolution of motional sidebands in sideband cooling requires a Rabi frequency $\Omega \ll \nu$. Therefore the trapping frequency necessarily limits the cooling rate and thus the achievable cooling rates are a few orders of magnitude lower than the trap frequency (see [13–15] for a more detailed discussion of the limits imposed on known cooling schemes).

We here present a fundamentally novel way of cooling a system of trapped particles, achieving rates that are faster than the trapping frequency, and which grows with the laser intensity, limited only by the time required to dissipate the energy from the ion's internal state—a time scale orders of magnitude faster than the trap frequency. We present the theoretical ideas underlying this scheme and demonstrate their feasibility by means of detailed numerics for the example of a linear ion trap. We show in detail how, using optimized sequences of coupling pulses, rapid cooling can be achieved. The proposed method is robust to fluctuations in the laser power and timing and to imperfect dissipative cooling. Moreover, it may be adapted to a very wide range of systems, such as for neutral atoms [7], trapped ions at low temperature [16], and mechanical oscillators [11,12], for which the method can break the final temperature limit imposed by the finite Q factor.

The superfast cooling concept.—Consider a trapped system which is coupled to a TLS. The system is in an almost-harmonic potential, with engineered coupling between the internal and external DOFs. For a standing wave configuration where the ion or atom is at the node we obtain in leading order of η the following Hamiltonian:

$$H/\hbar = \delta\sigma_z + \nu a^\dagger a + \eta\Omega(a^\dagger + a)\sigma_\theta, \qquad (1)$$

where δ is the laser detuning, η is the Lamb-Dicke parameter, ν is the trapping frequency, Ω is the effective Rabi coupling between the two internal levels, a is the phononic annihilation operators, and σ_θ is the pseudo spin operator in the direction θ in the x, y plane. To cool the system, we would like to transfer energy from the motional to the internal DOF., which can be dissipatively reinitialized via optical pumping. In other words, we wish to implement the red-sideband cooling operator, $a\sigma^+ + a^\dagger\sigma^-$, [13–15]. In sideband cooling this term is generated from the $\hat{X}\sigma_x$ term after a rotating wave approximation (RWA), which requires a time which is longer than the trapping frequency.

A natural question to ask is whether we can perform the coherent part of the cooling process, i.e., create the sidebandlike term, in times which are faster than the trap frequency. This question can be explored by numerical optimization over possible cooling sequences, but this requires an initial "point", i.e., a guess of the cooling

cycle, for one to have a reasonable chance of the optimization process succeeding. One may try to initiate the optimization with the schemes valid for the weak coupling regime such as sideband cooling or the Dark state cooling schemes and extend them to strong couplings. This approach proves unsuccessful. In our work we approach the problem from the opposite direction: we choose as our initial guess a cooling scheme in the impulsive limit (coherent manipulation is infinitely fast, neglecting higher order terms in the Hamiltonian), where we could reach the phononic ground state in the time it takes to reset the TLS to its ground state due to spontaneous emission. Starting from this point we optimize numerically to adapt to finite couplings attainable in the lab.

We start by discussing the idealized case to gain insight into the optimization procedure. Cooling at the strong-coupling limit is simple and extremely fast. We choose to start with the following argument, which elucidates the underlying intuition of our work: The sideband cooling term can be written as $a\sigma^+ + a^\dagger\sigma^- = \sqrt{\frac{m\omega}{2\hbar}}(\hat{X}\sigma_x - \frac{1}{m\omega}\hat{P}\sigma_y)$. We already have a $\hat{X}\sigma_x$ coupling available to us (1). Thus if we can create a $\hat{P}\sigma_y$ term, we can generate the red-sideband Hamiltonian using the Trotter decomposition [17]. Neglecting some constants, $(e^{i\Omega\hat{X}\sigma_x dt}e^{i\Omega\hat{P}\sigma_y dt})^n = e^{i(\hat{X}\sigma_x - \hat{P}\sigma_y)\Theta}$ when $dt \to 0$ and $\Omega n dt = \Theta$; i.e., multiple short pulses of $\hat{X}\sigma_x$ and $\hat{P}\sigma_y$ will be equivalent to time evolution according the desired $\hat{P}\sigma_y$ Hamiltonian. Therefore, if we had infinitely strong lasers and the $\hat{P}\sigma_y$ interaction, then at $\Theta = \pi$ the cooling rate would almost approach the TLS dissipation time scale.

$\hat{P}\sigma_y$ *term.*—Following the insight first described in [18] we derive $\hat{P}\sigma_y$ as an effective Hamiltonian using $\hat{X}\sigma_y$ pulses which give the ion momentum, a period of free evolution in which the ion translates and, finally, a $-\hat{X}\sigma_y$ pulse, imparting equal and opposite momentum, stopping the translation. Furthermore, in the strong-coupling regime the coupling is much larger than the phonon energy, $\eta\Omega \gg \nu$, allowing us to ignore the free evolution for the duration of the pulses. Setting $\delta = 0$ yields a solvable Hamiltonian which enables us to get an exact result. Formally, splitting (1) into $H_{\text{free}} = \hbar\nu(a^\dagger a + \frac{1}{2})$ and $H_{\text{pulse}} = \hbar\Omega\eta(a^\dagger + a)\sigma_y$, setting δ to zero and making use of the Baker-Campbell-Hausdorff formula [19] we get a closed-form expression

$$e^{(-i/\hbar)(t_f H_{\text{free}} + \hbar\eta t_f t_p \Omega\nu\hat{P}\sigma_y + \hbar\eta^2\nu\Omega^2 t_f t_p^2)}, \quad (2)$$

which includes the desired $\hat{P}\sigma_y$ operator, with t_p being the pulse duration and t_f the free evolution time, for the demi pulse. We can now combine a $\hat{X}\sigma_x$ pulse with a $X\sigma_y$-wait-$X\sigma_y$ sequence, implementing a $\hat{P}\sigma_y$ pulse and generate a red-sideband operator. Note that we have a large phase term $\hbar\eta^2\nu\Omega^2 t_f t_p^2$ that will need to be dealt with.

Results.—As the $\hat{P}\sigma_y$ interaction shifts the location of the ion it cannot be performed instantaneously. Moreover,

the true impulsive limit $H_{\text{free}} \ll H_{\text{pulse}}$ is not currently accessible in the lab and therefore we cannot completely ignore free evolution while pulsing. As a result, while the above approach provides us with a framework and a starting point, we must employ quantum optimal control techniques, the details of which are achieved through numerical optimization, to apply the above methods for finite pulse lengths and finite coupling strength. The pulses were optimized to give the lowest possible average number of phonons after cooling, starting from a number of initial temperatures. Note that the sequences presented here are just examples of what is achievable, and by no means are they to be considered canonical or globally optimal.

Numerical studies for this work have been performed using QLIB [20], a MATLAB package for quantum-information and quantum-optics calculations.

All computations below are done for the following physical settings, which are achievable in the lab: $^{40}\text{Ca}^+$, $\nu = 1\text{ MHz} \cdot 2\pi$, $\Omega = 100\text{ MHz} \cdot 2\pi$, $\lambda_{\text{laser}} = 730\text{ nm}$, giving a Lamb-Dicke value of $\eta = 0.31$, [21]. Table I details 3 sample cycles and their cooling performance. Note that the coupling terms in the resulting Hamiltonian are proportional to $t_p\eta\sqrt{\frac{2m\nu}{\hbar}}\Omega\hat{X}\sigma_\theta$ and $\eta t_f t_p\Omega\nu\hat{P}\sigma_y$ and therefore total coherent manipulation time scales as $1/\sqrt{\Omega}$, since $t_p \times t_f$ scales like $1/\Omega$, while the time requires for dissipative cooling remains unchanged.

The optimization was performed in the impulsive limit, and then the deduced sequence was applied using the full Hamiltonian. The results are shown in Fig. 1. Starting from a thermal state of varying temperatures, the continuous lines show the final energy for a single application of a cooling cycle and the dashed lines show the result of 25 applications of the same cycle. The latter cannot be deduced directly from the former because the state is no longer thermal after one or more cooling cycles. Note that even though the sequences were optimized for a specific initial temperature, the cycles give a good cooling for a wide range of initial temperatures.

In Fig. 2 we show how repeated applications of the three sample cycles continue to lower the energy, until a steady

TABLE I. Cooling cycle performance. We define a cooling sequence as a series of alternating $\hat{X}\sigma_x$ pulses and $\hat{P}\sigma_y$ demi pulses of varying lengths, followed by a reinitialization of the ion's internal DOF. A cooling cycle is comprised of several cooling sequences, which are generally nonidentical.

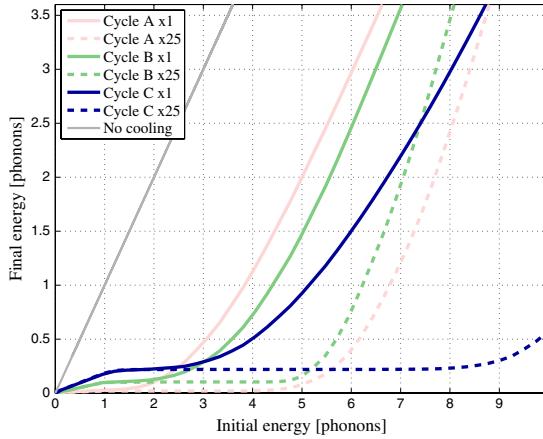|	Cycle A	Cycle B	Cycle C
Initial energy [$\hbar\nu$]	3	5	7
Final energy [$\hbar\nu$]	0.4	1.27	1.95
Final energy after 25 cycles	0.02	0.10	0.22
Duration of coherent operations	$4.4\frac{2\pi}{\nu}$	$2.7\frac{2\pi}{\nu}$	$0.8\frac{2\pi}{\nu}$
Total duration	$5.0\frac{2\pi}{\nu}$	$3.3\frac{2\pi}{\nu}$	$1.4\frac{2\pi}{\nu}$
No. pusles per cycle	180	90	90
No. of sequences	10	10	10

FIG. 1 (color online).　Initial and final energy (above ground, in units of $\hbar\nu$) for a single application of the cooling cycle and for 25 applications (mean over 1000 runs). Cycle A light (pink), cycle B midtone (green), cycle C dark (blue).

state, specific to each sequence, is achieved. An example timing of sequences within a cycle is shown in Fig. 2 inset, with the darkest area (blue) corresponding to X pulses, gray areas (red) corresponding to emulated P pulses and light areas to the ion's reinitialization.

Robustness.—The robustness of the cooling pulses is extremely important for experimental realization. In order to analyze the robustness we have simulated the operation of the pulses under noisy conditions of the lasers. The results indicate that the cooling pulses are extremely robust even though they were not optimized to be so. In Fig. 3 we study the robustness of cycle C, repeated 25 times, to Gaussian noise in the pulse timings. We assume that instead of the prescribed pulse time t, we implement $t \to (1 + \epsilon)t$, with ϵ being drawn from a Gaussian distribution with a varying standard deviation. A similar noise pattern was applied to the laser power, Ω. The superfast cooling

exhibits two slightly different sensitivities to noise: for the short time frame ($\ll \nu^{-1}$), which interferes with the commutation relations allowing the creation of the effective P pulse, sensitivity is somewhat higher, while for noise occurring on longer time scales, i.e., the duration of the various pulses comprising the cooling sequence, superfast cooling is extremely robust. The plots show the mean final phonon count over 500 cycles. A graceful degradation in cooling performance can be observed.

Note that the state of the system after cooling is not a thermal state. This is due partly to purely numerical issues and partly a physical feature of the specific cooling sequences presented (which itself stems from numeric limitations of the optimization process). The latter results in effective cooling operators that do not cool the high harmonic modes (above 30) as well as they cool lower modes. While this difference is negligible before cooling, when going significantly below 1 phonon, the remaining energy in the high modes becomes a not-insignificant part of the overall energy. We believe that with higher computational power sequences resulting is more thermal-like final states are achievable which would increase the efficiency of proposed cooling scheme.

Imperfect dissipative cooling.—For the purposes of the calculations above, we assumed a 10×30 ns cooling window, which is sufficient to provide negligible residual population in electronic states outside the cooling transition. We have also explored shorter cooling windows, taking into account off-resonant electronic levels as well as inadvertent heating. Using the numerical technique of quantum jumps [22,23], we have confirmed that degradation in cooling performance with decreasing length of the cooling window is gradual. Further optimization is hence expected to allow for future shortening of the overall cooling process. *Recoil term:* In the proposed cooling scheme the contribution of the recoil term is η^2 was
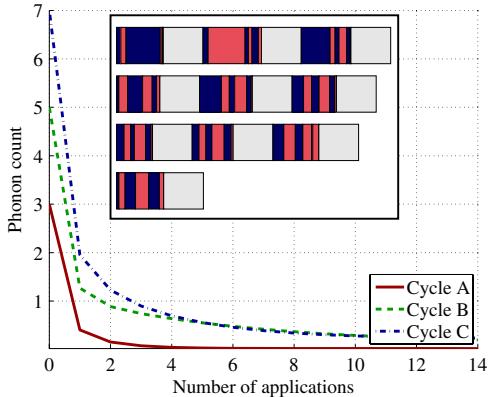

FIG. 2 (color online).　Cooling performance in repeated applications of the sample cycles. Inset: Representation of a cooling cycle. Each block of 6 bars [3 X (darker, blue) and 3 P pulses (lighter, pink)] representing a single cooling sequence. The sequences are interspaced by period for reinitialization of the ion's internal state. All together these make up a complete cooling cycle.
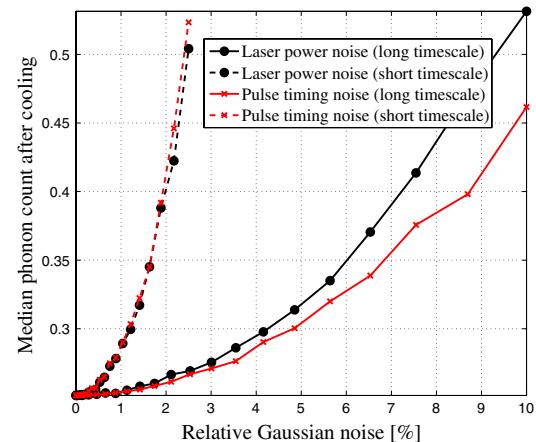

FIG. 3 (color online).　Robustness to noise of cooling cycle C, applied 25 times. The x axis represents the relative noise and the y axis the final phonon population. As can be seen, superfast cooling is proven to be quite robust, both at long (ν) and short ($\ll \nu$) time scales.

ignored due to numerical issues. This term is smaller then the cooling term, and thus the contribution to the final temperature and any possible degradation of the cooling performance will be relatively small; i.e., it will limit the final population at around η^2.

Ion chain.—By applying this cooling method to each individual ion in a large ion chain, we create a product state of individual ions' ground states, i.e., we will cool to the $|0\rangle|0\rangle \dots |0\rangle$ state in the local basis—which is not the global ground state. For chains of moderate size placed in the $|0\rangle|0\rangle \dots |0\rangle$ state, we see that the number of phonons in the collective center of mass (COM) mode is $0.073N$–0.122 phonons for chains in which the ions are not equidistant, and up to 0.092 phonons for equidistant chains (asymptotic value). Note that the COM phonon population is low for both cases, even for moderate chains. Thus, cooling a chain to a product of individual ions' ground states is a very good approximation of the global ground state.

Standing wave.—Note that we are interested here in the pulsed application of a standing wave, which can be emulated using running wave pulses by using the two following pulses: $i\Omega(\sigma_x + \eta\sigma_y x)$, $-i\Omega(\sigma_x - \eta\sigma_y x)$. These pulses can be created by passing an initial pulse through a beam splitter and bringing it together from two opposite directions, thus controlling the phase and sign of the Lamb-Dicke parameters independently. This is described by the unitary transformation $e^{i\Omega\sigma_x}e^{i\eta\Omega\sigma_y x}e^{-i\Omega\sigma_x}e^{i\eta\Omega\sigma_y x} \approx e^{i2\eta\Omega\sigma_y x}$, which creates the unitary operation that is required. Moreover, as we are interested in very fast processes, we can be sure that the standing wave will not drift. Also, see [24] for creation of standing waves.

So far we have assumed that the ion can be modeled by a nondissipative two-level system with effective Rabi frequency Ω—an obvious simplification. Some experimental setups use a three-level system with the effective Rabi cycle achieved by way of a highly detuned Raman transition off a highly-dissipative level [13–15]. As a result, the true laser coupling of 100 GHz is reduced to an effective coherent 10 MHz transition. However, unlike quantum-information processing, superfast cooling does not require a fully coherent transition. We could reduce the detuning and achieve a higher Rabi frequency. Thus, given sufficiently strong lasers the overall time of the cooling process could potentially be reduced to the time required for dissipative cooling (with appropriate optical repumping, as needed), reducing the coherent manipulation time towards zero.

Nanomechanics.—The cooling scheme presented here may have increasing importance for nanomechanical systems where the finite Q value limits the final temperature. One would use the setup described in [11,12], i.e., couple a TLS to the oscillator. In this case the effective Lamb-Dicke parameter is on the order of $\eta = 0.03$ ([12]) and can be much higher for the scheme which is generated with magnetic gradients ([11]). In both of these schemes the strong-

coupling regime can be reached by strong lasers or even microwaves. The method currently in use [25,26], assisted by a cavity, cannot beat the limit of the trap frequency due to the Gaussian nature of the scheme.

Conclusion.—An optimized-control approach to cooling trapped ions has been introduced, by optimizing over the realizable couplings between the phonons and the ion's internal levels, $\hat{X}\sigma_\theta$, and over the periods of free evolution. Surprisingly, even this basic set is sufficient to implement a red-sideband-like operation and drive energy from the phonons to the ions, at a rate higher than the trapping frequency. Furthermore, the principles described above are applicable to a very wide range of system and robust enough to be implementable in ongoing experiments.

[1] T. W. Hänsch and A. L. Schawlow, Opt. Commun. **13**, 68 (1975).

[2] D. Wineland and H. Dehmelt, Bull. Am. Phys. Soc. **20**, 637 (1975).

[3] P. Lett *et al.*, Phys. Rev. Lett. **61**, 169 (1988).

[4] J. Dalibard and C. Cohen-Tannoudji J. Opt. Soc. Am. B **6**, 2023 (1989).

[5] D. J. Wineland *et al.*, J. Opt. Soc. Am. B **9**, 32 (1992).

[6] A. Aspect *et al.*, J. Opt. Soc. Am. B **6**, 2112 (1989).

[7] M. Kasevich and S. Chu Phys. Rev. Lett. **69**, 1741 (1992).

[8] G. Morigi *et al.*, Phys. Rev. Lett. **85**, 4458 (2000).

[9] C. Monroe *et al.*, Phys. Rev. Lett. **75**, 4011 (1995).

[10] J. Cerrillo, A. Retzker, and M. B. Plenio, Phys. Rev. Lett. **104**, 043003 (2010).

[11] P. Rabl *et al.*, Phys. Rev. B **79**, 041302 (2009).

[12] I. Wilson-Rae, P. Zoller, and A. Imamoglu, Phys. Rev. Lett. **92**, 075507 (2004).

[13] D. J. Wineland, R. E. Drullinger, and F. L. Walls, Phys. Rev. Lett. **40**, 1639 (1978).

[14] C. Monroe *et al.*, Phys. Rev. Lett. **75**, 4011 (1995).

[15] V. Vuletic *et al.*, Phys. Rev. Lett. **81**, 5768 (1998).

[16] D. Leibfried *et al.*, Rev. Mod. Phys. **75**, 281 (2003).

[17] M. Suzuki, Physica (Amsterdam) **194A**, 432 (1993).

[18] A. Retzker, J. I. Cirac, and B. Reznik, Phys. Rev. Lett. **94**, 050504 (2005).

[19] M. W. Reinsch, J. Math. Phys. (N.Y.) **41**, 2434 (2000).

[20] S. Machnes, arXiv:0708.0478, http://qlib.info.

[21] T. Monz *et al.*, Phys. Rev. Lett. **103**, 200503 (2009).

[22] Mølmer *et al.*, J. Opt. Soc. Am. B **10**, 524 (1993).

[23] M. B. Plenio and P. L. Knight, Rev. Mod. Phys. **70**, 101 (1998).

[24] The mirror can be mounted to the electrodes of the ion trap as currrnetly done in the Ion trap group in Ulm. Private communication with Kilian Singer.

[25] I. Wilson-Rae *et al.*, Phys. Rev. Lett. **99**, 093901 (2007).

[26] F. Marquardt *et al.*, Phys. Rev. Lett. **99**, 093902 (2007).